ACS APPLIED BIO MATERIALS Article
Cite This: ACS Appl. Bio Mater. 2018, 1, 777−782
www.acsabm.org

# Ascorbic Acid-Loaded Apoferritin-Assisted Carbon Dot-$MnO_2$ Nanocomposites for the Selective and Sensitive Detection of Trypsin

Qingqing Tan,[∥,†] Ruirui Zhang,[∥,‡] Weisu Kong,[†] Fengli Qu,[*,†] and Limin Lu[*,§]

[†]College of Chemistry and Chemical Engineering, Qufu Normal University, Qufu, Shandong 273165, People's Republic of China
[‡]Beijing Key Laboratory of Ionic Liquids Clean Process, CAS Key Laboratory of Green Process and Engineering, Institute of Process Engineering, Chinese Academy of Sciences, Beijing 100190, People's Republic of China
[§]Institute of Functional Materials and Agricultural Applied Chemistry, College of Science, Jiangxi Agricultural University, Nanchang 330045, People's Republic of China

Supporting Information

**ABSTRACT:** A novel "turn-on" fluorescent trypsin detection platform dependant on carbon dot-$MnO_2$ (CD-$MnO_2$) nanocomposites and ascorbic acid-loaded apoferritin (APOAA) was fabricated. The detection mechanism relied on trypsin-catalyzed enzymolysis of APOAA, which released ascorbic acid (AA) as a reducing agent to disintegrate the $MnO_2$ nanosheets, causing the recovery of the fluorescence of CDs. An excellent performance and high sensitivity of trypsin determination were observed with a detection limit (LOD) of 0.3411 ng/mL. This work provides us with a unique strategy for trypsin detection in human serum samples, which reveals the potential applications in clinical detection.

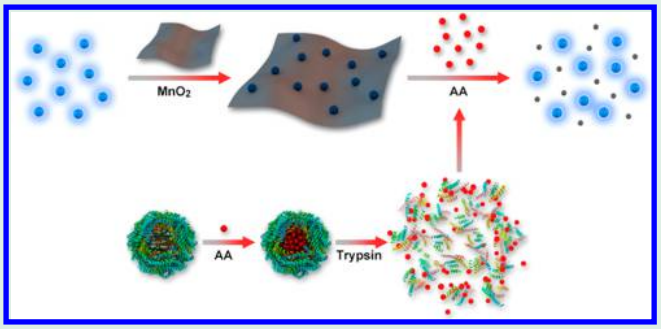


**KEYWORDS:** *fluorescence, carbon dots, $MnO_2$ nanosheets, apoferritin, trypsin, fluorescence resonance energy transfer*

## 1. INTRODUCTION

Trypsin is a key alkaline protease, which widely exists in many vertebrates' digestive systems, and is able to cleaving peptides at the C-terminal side of arginine or lysine residues.[1−4] Besides, trypsin is of importance in regulating the pancreatic exocrine function, and its imbalance will lead to many diseases, like pancreatitis, vesicular fibrosis, pancreatic carcinoma, etc.[5−7] The level of trypsin in urine or serum is regarded as a biomarker for the diagnosis of pancreatic diseases.[8] Consequently, accurate detection of trypsin with a high selectivity and low detection limit exhibits a vital clinical diagnosis and therapeutic significance. So far, many methods have been reported for detecting trypsin activity, such as the mass spectrometry,[9] enzyme-linked immunosorbent assay (ELISA),[10] gel electrophoresis,[11] electrochemical analysis,[12] chemiluminescence spectrometry,[13,14] photoelectrochemistry analysis,[15] colorimetric spectrometry,[16−18] and fluorescence spectrometry.[19−21] Among that, fluorescence spectroscopy has gained a lot of attention on account of its low background noise, high sensitivity, and easy operation. The fluorescent determination of trypsin on the basis of quantum dots and Au nanoclusters has been reported in the past.[19,20] However, current methods are still plagued with several problems, such as the toxicity of quantum dots, the insensitivity of "turn-off" detection, and the requirement of numerous reagents.[4,19,22] To this end, the detection strategy of trypsin still requires technique improvement to offer an effective practical assessment.

Carbon dots (CDs) have recently attracted considerable interests resulting from their excellent photostability, low toxicity, easily fabrication, favorable biocompatibility, and good aqueous solubility.[23,24] In particular, the fluorescence of CDs could be quenched by $MnO_2$ nanosheets via fluorescence resonance energy transfer (FRET). $MnO_2$ nanosheets with a wide absorption range from 250 to 600 nm exhibit a major peak at 374 nm, making them serve as an efficient quencher.[25,26] Additionally, owing to the strong oxidation ability, $MnO_2$ nanosheets could be decomposed to $Mn^{2+}$ by ascorbic acid (AA).[24] Herein, we proposed a strategy that protein cage encapsulated AA was enzymatically hydrolyzed; releasing AA would lead to the disintegration of $MnO_2$, which realized the sensitive detection of a specific enzyme in an indirect way. It has been reported that apoferritin (APO) could load AA via an assembly−disassembly method and could also be catalytically hydrolyzed by trypsin.[7] Therefore, ascorbic acid-loaded apoferritin (APOAA) could be utilized as an assistant agent and then combined with CD-$MnO_2$ nanocomposites for the detection of trypsin.

Received: June 15, 2018
Accepted: August 24, 2018
Published: August 24, 2018






DOI: 10.1021/acsabm.8b00235
ACS Appl. Bio Mater. 2018, 1, 777−782

**Scheme 1. Schematic Illustration of Quantitative Trypsin Detection**

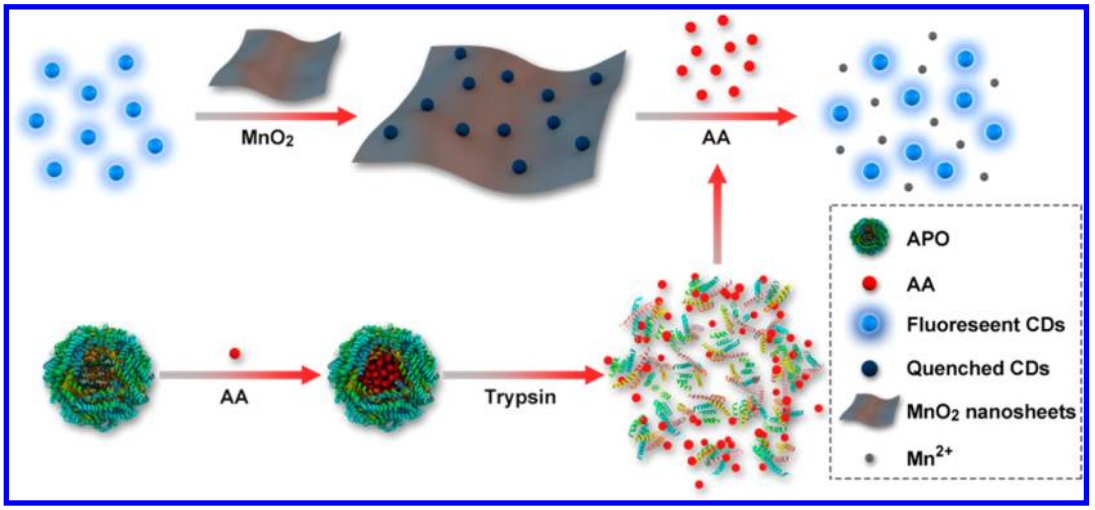


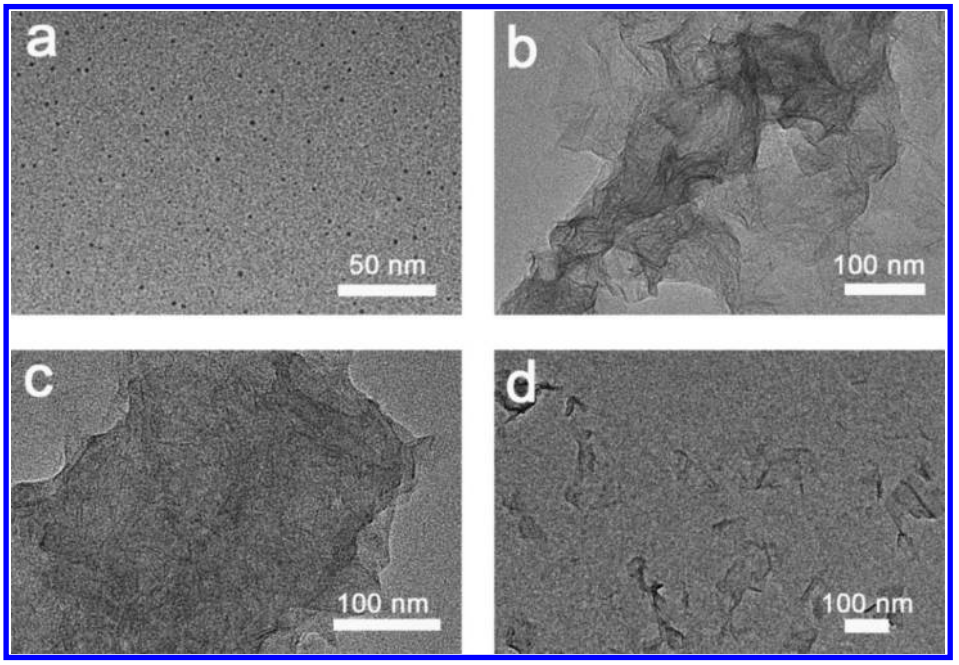


**Figure 1.** TEM images of (a) CDs, (b) $MnO_2$ nanosheets, (c) CD-$MnO_2$ nanocomposites, and (d) disaggregated $MnO_2$ nanosheets.

In this work, we prepared CD-$MnO_2$ nanocomposites by electrostatic interaction and designed the CD-$MnO_2$-APOAA system (CMA) for trypsin detection. APOAA was used as a bifunctional agent for both the storage of AA and enzymatic substrate of trypsin. After the APOAA was catalytically hydrolyzed by trypsin, the released AA would reduce $MnO_2$ to $Mn^{2+}$. Then, the $MnO_2$ nanosheets were destroyed, which resulted in the fluorescence recovery of CDs. Therefore, by evaluating the fluorescence intensity of CDs, a sensitive detection platform for the determination of trypsin was established.

## 2. EXPERIMENTAL SECTION

**2.1. Reagents and Materials.** Sterculia lychnophora was obtained from Tongrentang Medicine Cooperation (China). HCl and NaOH were bought from Sinopharm Chemical Reagent Co., Ltd. (China). Ascorbic acid (AA), bovine serum albumin (BSA), bovine hemoglobin (Hb), and human serum albumin (HAS) were supplied from Aladdin Chemical (China). Tetramethylammonium hydroxide, manganese chloride tetrahydrate ($MnCl_2{\cdot}4H_2O$), apoferritin (APO), glucose (Glu), alkaline phosphatase (ALP), glucose oxidase (GOx), pepsin, and trypsin were purchased from Sigma-Aldrich (USA). Phosphate buffer solution (PBS, pH = 7.8) was applied for trypsin incubation and fluorescent detection. All reagents were analytical grade and used directly. The solutions were prepared with deionized water.

**2.2. Preparation of APOAA.** The APOAA was prepared via the assembly−disassembly method documented in previous reports with a minor modification.[15,27] APOAA is prepared by adjusting the pH for loading AA into APO. (The details are in the Supporting Information.) The gained APOAA was saved in brown bottles for further experiments.

**2.3. Preparation of CD-$MnO_2$ Nanocomposites.** The CDs were synthesized according to a hydrothermal method described in our previous report.[24] In brief, sterculia lychnophora was peeled and ground to get sterculia lychnophora seed powder. Afterward, the powder was dissolved in $H_2O$, and the mixture proceeded via the hydrothermal process of heating for 1 h at 100 °C. Then the gained CDs in solution were filtered with a 0.22 $\mu$m filtration membrane and kept in a dark room for the next steps. Next, the $MnO_2$ nanosheets



DOI: 10.1021/acsabm.8b00235
ACS Appl. Bio Mater. 2018, 1, 777−782

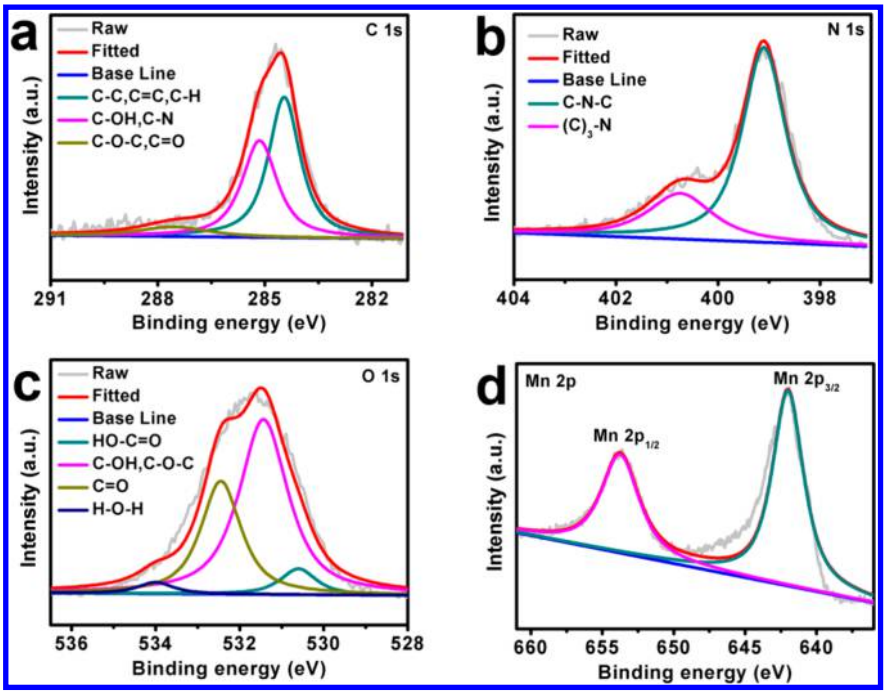


**Figure 2.** XPS spectra of CDs-$MnO_2$ in the (a) C 1s, (b) N 1s, (c) O 1s, and (d) Mn 2p regions.

were prepared by referring to the literature.[28] The details are in the Supporting Information.

Finally, the CD-$MnO_2$ nanocomposites were prepared as follows: 200 $\mu$L of various concentrations of $MnO_2$ nanosheet solutions was mixed with 200 $\mu$L of CDs solution. The total volume of the CD-$MnO_2$ solution was adjusted to 1 mL using PBS buffer for the next analysis.

**2.4. Detection of Trypsin.** For detecting trypsin, in detail, 100 $\mu$L of APOAA was added into CD-$MnO_2$ nanocomposites to prepare CMA. Afterward, 100 $\mu$L of trypsin at various concentrations was mixed with the aforementioned CMA solution, and the mixture was incubated for 15 min at 37 °C. Finally, the fluorescent signal of CMA was recorded over a range from $\lambda$ = 320 nm to $\lambda$ = 680 nm.

## 3. RESULTS AND DISCUSSION

**3.1. Principle of Detection.** A novel fluorescence turn-on method for detecting trypsin activity in a homogeneous system was successfully developed based on an enzyme-catalyzed in situ release of AA. The principle of the detection was displayed in Scheme 1. The freshly synthesized negatively charged $MnO_2$ nanosheets can easily adsorb on the surface of aminated CDs through electrostatic interaction. The formation of CD-$MnO_2$ nanocomposites could efficiently cause the fluorescence quench of CDs via FRET. In particular, the APOAA prepared via the assembly−disassembly method could be catalytically hydrolyzed by trypsin to release AA. Then the released AA would destroy the structure of $MnO_2$ nanosheets by reducing $MnO_2$ to $Mn^{2+}$, yielding the recovered fluorescence of the CDs. It is remarkable to point out that the mechanism relied on the fluorescence changes caused by hydrolysis of APOAA, thus realizing the detection of trypsin according to monitoring the fluctuation of the CD fluorescence intensity.[29]

**3.2. Characterization and Feasibility.** The morphology, size, and microstructure of synthesized nanomaterials were observed by the transmission electron microscopy (TEM) images. As shown in Figure 1a, the prepared CDs are uniform and monodispersed with a quasi-spherical shape. Figure 1b shows a typical TEM image of $MnO_2$ nanosheets, which presents an obvious 2D sheet structure with occasional folds and wrinkles. Figure 1c manifests CD-$MnO_2$ nanocomposites were successfully formed by electrostatic interaction between negative $MnO_2$ nanosheets and aminated CDs. The $MnO_2$ nanosheets could be disintegrated by the reduction of AA, which was released from APOAA by adding trypsin. Successful reduction of $MnO_2$ to $Mn^{2+}$ was confirmed by Figure 1d. Figure S1a displays the TEM image of APOAA. APOAA has a nanocage structure with an interior and exterior diameter of 8 ± 1.2 nm and 12 ± 1.5 nm, which is similar with the pure apoferritin.[30] As shown in Figure S1b, the $\zeta$ potentials of APO and APOAA are −17.9 ± 1 mV and −12.9 ± 0.5 mV, respectively.

In addition, X-ray photoelectron spectroscopy (XPS) was employed to determine the elemental analysis and surface composition of CDs-$MnO_2$. The full XPS survey spectrum of CDs-$MnO_2$ (Figure S2) indicates the existence of C, O, N, and Mn elements. The C 1s spectrum in Figure 2a indicates three peaks at 284.2 eV ($sp^3$), 285.3 eV ($sp^3$), and 287.2 eV ($sp^2$), which are ascribed to the C—C, C═C; C—H, C—N/C—OH; and C═O/C—O—C, respectively. The N 1s spectrum (Figure 2b) confirms that the peaks at 399.3 eV and 400.6 eV are corresponding to C—N—C and $(C)_3$—N, respectively. The O 1s spectrum (Figure 2c) exhibits four peaks at 530.2, 531.3, 532.5, and 534.1 eV, respectively. The Mn 2p spectrum (Figure 2d) shows two peaks located at 642.0 and 653.9 eV, and they are assigned to Mn $2p_{3/2}$ and Mn $2p_{1/2}$, respectively. These results are in accord with the previous reports.[31,32]

The optical properties of CDs and $MnO_2$ nanosheets were also investigated by UV−vis absorbance and fluorescence spectra. The red dotted line in Figure 3 shows that CDs have a UV absorption peak at 345 nm and exhibit a strong blue emission peak at 455 nm (black solid line). It should be pointed out that the absorption spectrum of $MnO_2$ exhibits a wide band ranging from 270 to 600 nm (black dotted line), which overlaps basically with the fluorescence emission


DOI: 10.1021/acsabm.8b00235
ACS Appl. Bio Mater. 2018, 1, 777−782

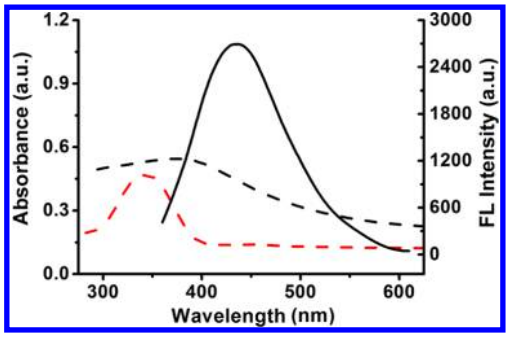


**Figure 3.** UV spectra of CDs (red dotted line) and $MnO_2$ nanosheets (black dotted line) as well as the fluorescence emission spectrum of CDs (black solid line).

spectrum of CDs and thus can act as an ideal energy acceptor.[33]

The stability of $MnO_2$ was investigated by the $\zeta$ potentials of $MnO_2$ nanosheets at different periods. Figure S3 shows that the $\zeta$ potential of newly synthesized $MnO_2$ nanosheets is $-41.1 \pm 1$ mV and that the $\zeta$ potential of $MnO_2$ nanosheets stored for 6 months is $-39.9 \pm 0.5$ mV, which proved that the $MnO_2$ nanosheets is stable.

To further demonstrate the feasibility of the proposed strategy for trypsin detection, the fluorescence spectra measurement was performed. As shown in Figure 4, the

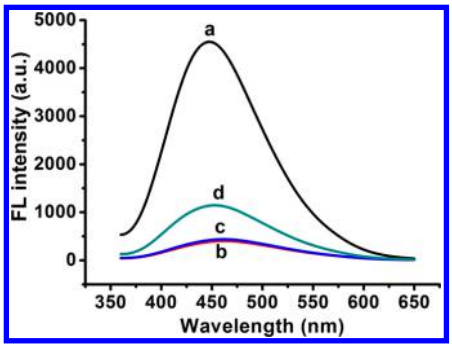


**Figure 4.** Fluorescence emission spectra of (a) CDs, (b) CD-$MnO_2$ nanocomposites, (c) CMA in the absence of trypsin, and (d) CMA in the presence of trypsin.

prepared CDs exhibit a strong fluorescence emission peak at 455 nm (line a in Figure 4), which could be quenched by $MnO_2$ nanosheets based on FRET (line b in Figure 4). The fluorescence of CD-$MnO_2$ nanocomposites would not be influenced by APOAA because the AA could be fully confined in APOAA (line c in Figure 4). With the addition of trypsin, the fluorescence of CMA is recovered (line d in Figure 4). Trypsin could catalytically hydrolyze APOAA to release AA. Consequently, $MnO_2$ nanosheets would be reduced into $Mn^{2+}$ and disintegrate rapidly, which contributed to the recovery of the fluorescence of CDs.

**3.3. Optimization of Detection Parameters.** To get the excellent detection performance, we explored the effects of various conditions including $MnO_2$ concentration, reaction pH, time, and temperature. The aforementioned parameters, which might affect the fluorescence signal response of CMA, were necessary to be optimized.

The concentration of $MnO_2$ is highly significant for designing CMA, which would be first investigated. $MnO_2$ nanosheets with various concentrations were added into 200 $\mu$L of the CD solution, followed by adding APOAA and trypsin. Subsequently, the fluorescence recovery value, $F - F_0$, of CMA was recorded. ($F$ and $F_0$ represent the fluorescence intensities of CMA in the presence and absence of trypsin, respectively.) As shown in Figure S4a, the $F - F_0$ value rapidly enhances with the increased $MnO_2$ nanosheet concentration from 0 to 40 $\mu$g/mL, reaching a maximum value at 40 $\mu$g/mL and then the signal decreasing with the further increase of the $MnO_2$ nanosheet concentration. The reason for this phenomenon is mainly that APOAA can only load a deterministic amount of AA so that the release of AA could not completely disintegrate $MnO_2$ nanosheets when $MnO_2$ nanosheets are present at a high concentration. Therefore, based on the above results, the optimal $MnO_2$ nanosheet concentration (40 $\mu$g/mL) was selected for the further detection.

In addition, the effect of pH was explored by varying PBS (pH = 7.0, 7.5, 7.8, 8.0, 8.5, and 9.0). As shown in Figure S4b, at the pH of 7.8, $F - F_0$ displays the maximum, which illustrated that trypsin exhibits a maximum proteolytic activity at this pH. Then pH 7.8 was chosen for the further assay. The reaction time between CMA and trypsin is also an important parameter, as demonstrated in Figure S4c; $F - F_0$ increased gradually within 15 min and then reaches to a stable stage during the following 30 min. Thus, 15 min was chosen as the optimized reaction time for the following studies. Reaction temperature, a critical aspect that affects enzyme activity, was also investigated, and the results were shown in Figure S4d. After trypsin was added into the CMA solution, $F - F_0$ increases with the increasing temperature from 25 to 37 °C,

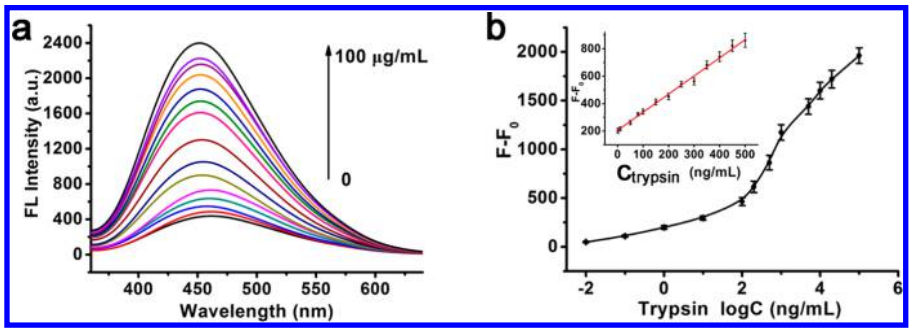


**Figure 5.** (a) Fluorescence emission spectra of CMA in the presence of various trypsin concentrations (0–100 $\mu$g/mL). (b) Relationship between the fluorescence recovery value $F - F_0$ of CMA and the trypsin concentration. The inset graph shows a linear standard plot between the fluorescence recovery value and the trypsin concentration. (The letter "C" in log $C$ means the trypsin concentration. $F_0$ and $F$ are the fluorescence intensities of CMA in the absence and presence of trypsin, respectively.)



DOI: 10.1021/acsabm.8b00235
ACS Appl. Bio Mater. 2018, 1, 777–782

while the fluorescence intensity decreases gradually by further increasing the temperature, which might be ascribed to the decrease of trypsin activity at higher temperatures. Therefore, 37 °C was chosen as the appropriate temperature for detecting trypsin.

**3.4. Performance for Trypsin Detection.** Under the optimized conditions, the performance of the current strategy for quantitative determination of trypsin was investigated. As illustrated in Figure 5a, the fluorescence peak of CMA located at 455 nm recovers gradually with the increasing concentrations of trypsin in the range 0−100 μg/mL. Figure 5b shows that $F - F_0$ exhibits an excellent linear relationship to the trypsin's concentrations ranging from 1 to 500 ng/mL, and the linear regression equation is $F - F_0$ = 1.3214 C (ng/mL) + 205.2248 ($R^2$ = 0.9932). The detection limit of trypsin was estimated to be 0.3411 ng/mL, according to the 3σ rule. These results demonstrate that the current strategy was more sensitive compared to most of the previous reported methods for trypsin determination (Table S1).

In addition to sensitivity, selectivity is another necessary factor for an originally designed detection system in order to apply it in a real sample for potential applications. To evaluate the specificity of the current detection system for trypsin, the fluorescent responses of CMA to trypsin and several potential interfering compounds (corresponding concentrations listed in Figure 6), including BSA, BH, HSA, glucose, ALP, GOx, and pepsin, were monitored. As shown in Figure 5, only trypsin could increase the fluorescence of CMA, while other proteins could not hydrolyze APOAA and thus lead to the release of AA. The result indicates that the designed fluorescence detection system indeed possesses a high selectivity toward trypsin, which may be directly applied to detect trypsin in real samples.

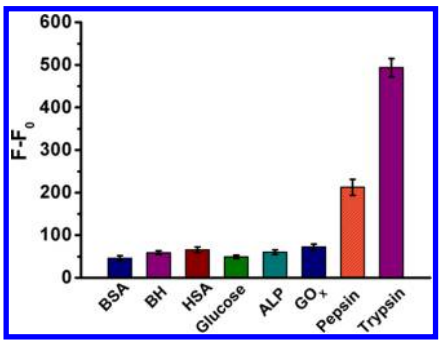


**Figure 6.** Selectivity of CMA for trypsin over other potential interferences. (The concentration of BSA, BH, HSA, and glucose is 10 μg/mL, and the concentration of ALP, $GO_x$, pepsin, and trypsin is 100 ng/mL.) The error bars were derived from the standard deviation of three measurements. Error bar = SD ($n$ = 3). $F_0$ and $F$ are the fluorescence intensities of CMA in the absence and presence of trypsin, respectively.

**3.5. Trypsin Detection in Serum Samples.** To explore the practical application of the developed detection system in complex biological samples (common concentration of trypsin in healthy human serum = 4.1−7.4 ng/mL),[34] the assay for trypsin detection in healthy human serum samples was conducted. The serums were provided by the People Hospital of Qufu. The experimental procedures were carried out by a standard addition method.[35] To be specific, $MnO_2$ nanosheet solution, CDs, and APOAA were mixed to prepare CMA. Afterward, a serum sample diluted 100 times was added into CMA solution for 15 min at 37 °C to measure the fluorescence. Next, trypsin with different concentrations was added in the mixed solution, and the mixture was incubated for 15 min to detect the fluorescence signal. From Table S2, it could be seen that the analytical recoveries ranges from 96% to 103%, which indicates that the developed method indeed has the potential applicability for detecting trypsin in real biological samples.

## 4. CONCLUSION

To sum up, we have developed a novel strategy to detect ultrasensitive trypsin based on the fluorescence "turn-on" of CMA. The detection mechanism is dependent on trypsin-catalyzed enzymolysis of APOAA, and the released AA acts as a reducing agent to disintegrate the $MnO_2$ nanosheets, resulting in the recovery of the fluorescence of CDs. The developed method for the detection of trypsin has a line range from 1 to 500 ng/mL with a detection limit of 0.3411 ng/mL. Moreover, the strategy exhibits excellent performance for trypsin detection in human serum samples, which revealed the potential applications in clinical detection.

## ■ ASSOCIATED CONTENT

### Supporting Information

The Supporting Information is available free of charge on the ACS Publications website at DOI: 10.1021/acsabm.8b00235.

Detailed information including experimental procedures; TEM and ζ potential of APOAA; XPS survey spectrum of CD-$MnO_2$ nanocomposites; ζ potential of $MnO_2$, dependence of the fluorescence recovery value of CMA on $MnO_2$ nanosheet concentration, reaction pH, reaction time, and reaction temperature; comparison of this method with the reports for trypsin determination; recovery results of the determination of trypsin in serum samples (PDF)

## ■ AUTHOR INFORMATION

### Corresponding Authors

*E-mail: fengliquhn@hotmail.com.
*E-mail: lulimin816@hotmail.com.

### ORCID

Fengli Qu: 0000-0001-6311-3051

### Author Contributions

‖Q.T. and R.Z. contributed equally to this work.

### Notes

The authors declare no competing financial interest.

## ■ ACKNOWLEDGMENTS

This work is supported by Beijing National Science Foundation (2174085), the National Natural Science Foundation of China (21775089 and 21705151), and the Outstanding Youth Foundation of Shandong Province (ZR2017JL010).

## ■ REFERENCES

(1) Zaccheo, B. A.; Crooks, R. M. Self-Powered Sensor for Naked-Eye Detection of Serum Trypsin. *Anal. Chem.* **2011**, *83*, 1185−1188.
(2) Liao, D.; Li, Y.; Chen, J.; Yu, C. A Fluorescence Turn-on Method for Real-Time Monitoring of Protease Activity Based on the Electron Transfer Between a Fluorophore Labeled Oligonucleotide and Cytochrome *c*. *Anal. Chim. Acta* **2013**, *784*, 72−76.



DOI: 10.1021/acsabm.8b00235
*ACS Appl. Bio Mater.* 2018, 1, 777−782

(3) Olsen, J. V.; Ong, S. E.; Mann, M. Trypsin Cleaves Exclusively C-Terminal to Arginine and Lysine Residues. *Mol. Cell. Proteomics* **2004**, *3*, 608−614.
(4) Wang, Y.; Li, J. A Carbon Nanotubes Assisted Strategy for Insulin Detection and Insulin Proteolysis Assay. *Anal. Chim. Acta* **2009**, *650*, 49−53.
(5) Zhang, L.; Du, J. A Sensitive and Label-Free Trypsin Colorimetric Sensor with Cytochrome *c* as a Substrate. *Biosens. Bioelectron.* **2016**, *79*, 347−352.
(6) Turk, B. Targeting Proteases: Successes, Failures and Future Prospects. *Nat. Rev. Drug Discovery* **2006**, *5*, 785−799.
(7) Chen, H.; Fang, A.; Zhang, Y.; Yao, S. Silver Triangular Nanoplates as an High Efficiently FRET Donor-Acceptor of Upconversion Nanoparticles for Ultrasensitive "Turn On-Off" Protamine and Trypsin Sensor. *Talanta* **2017**, *174*, 148−155.
(8) Shi, F.; Wang, L.; Li, Y.; Zhang, Y.; Su, X. A Simple "Turn-On" Detection Platform for Trypsin Activity and Inhibitor Screening Based On N-Acetyl-L-Cysteine Capped CdTe Quantum Dots. *Sens. Actuators, B* **2018**, *255*, 2733−2741.
(9) Fong, B. Y.; Norris, C. S. Quantification of Milk Fat Globule Membrane Proteins Using Selected Reaction Monitoring Mass Spectrometry. *J. Agric. Food Chem.* **2009**, *57*, 6021−6028.
(10) Seia, M. A.; Stege, P. W.; Pereira, S. V.; De Vito, I. E.; Raba, J.; Messina, G. A. Silica Nanoparticle-Based Microfluidic Immunosensor with Laser-Induced Fluorescence Detection for The Quantification of Immunoreactive Trypsin. *Anal. Biochem.* **2014**, *463*, 31−37.
(11) Lefkowitz, R. B.; Schmid-Schönbein, G. W.; Heller, M. J. Whole Blood Assay for Trypsin Activity Using Polyanionic Focusing Gel Electrophoresis. *Electrophoresis* **2010**, *31*, 2442−2451.
(12) Dong, M.; Qi, H.; Ding, S.; Li, M. Electrochemical Determination of Trypsin Using a Heptapeptide Substrate Self-Assembled on a Gold Electrode. *Microchim. Acta* **2015**, *182*, 43−49.
(13) Zhang, H.; Yu, D.; Zhao, Y.; Fan, A. Turn-On Chemiluminescent Sensing Platform for Label-Free Protease Detection Using Streptavidin-Modified Magnetic Beads. *Biosens. Bioelectron.* **2014**, *61*, 45−50.
(14) Zhang, Q.; Li, W.; Chen, J.; Wang, F.; Wang, Y.; Chen, Y.; Yu, C. An Ultrasensitive Chemiluminescence Turn-On Assay for Protease and Inhibitor Screening with a Natural Substrate. *Chem. Commun.* **2013**, *49*, 3137−3139.
(15) Chen, J.; Zhao, G. C. Nano-Encapsulant of Ascorbic Acid-Loaded Apoferritin-Assisted Photoelectrochemical Sensor for Protease Detection. *Talanta* **2017**, *168*, 62−66.
(16) Di, J.; Xia, J.; Ji, M.; Xu, L.; Yin, S.; Zhang, Q.; Chen, Z.; Li, H. Carbon Quantum Dots in Situ Coupling to Bismuth Oxyiodide via Reactable Ionic Liquid with Enhanced Photocatalytic Molecular Oxygen Activation Performance. *Carbon* **2016**, *98*, 613−623.
(17) Wang, G. L.; Jin, L. Y.; Dong, Y. M.; Wu, X. M.; Li, Z. J. Intrinsic Enzyme Mimicking Activity of Gold Nanoclusters Upon Visible Light Triggering and Its Application for Colorimetric Trypsin Detection. *Biosens. Bioelectron.* **2015**, *64*, 523−529.
(18) Ding, X.; Ge, D.; Yang, K. L. Colorimetric Protease Assay by Using Gold Nanoparticles and Oligopeptides. *Sens. Actuators, B* **2014**, *201*, 234−239.
(19) Li, X.; Zhu, S.; Xu, B.; Ma, K.; Zhang, J.; Yang, B.; Tian, W. Self-Assembled Graphene Quantum Dots Induced by Cytochrome c: a Novel Biosensor for Trypsin with Remarkable Fluorescence Enhancement. *Nanoscale* **2013**, *5*, 7776−7779.
(20) Hu, L.; Han, S.; Parveen, S.; Yuan, Y.; Zhang, L.; Xu, G. Highly Sensitive Fluorescent Detection of Trypsin Based on BSA-Stabilized Gold Nanoclusters. *Biosens. Bioelectron.* **2012**, *32*, 297−299.
(21) Li, N.; Li, Y.; Han, Y.; Pan, W.; Zhang, T.; Tang, B. A Highly Selective and Instantaneous Nanoprobe for Detection and Imaging of Ascorbic Acid in Living Cells and In Vivo. *Anal. Chem.* **2014**, *86*, 3924−3930.
(22) Li, J.; Hong, X.; Li, D.; Zhao, K.; Wang, L.; Wang, H.; Du, Z.; Li, J.; Bai, Y.; Li, T. Mixed Ligand System of Cysteine and Thioglycolic Acid Assisting in The Synthesis of Highly Luminescent Water-Soluble CdTe Nanorods. *Chem. Commun.* **2004**, *0*, 1740−1741.
(23) Cai, Q.; Li, J.; Ge, J.; Zhang, L.; Hu, Y.; Li, Z.; Qu, L. A Rapid Fluorescence "Switch-On" Assay For Glutathione Detection by Using Carbon Dots-$MnO_2$ Nanocomposites. *Biosens. Bioelectron.* **2015**, *72*, 31−36.
(24) Qu, F.; Pei, H.; Kong, R.; Zhu, S.; Xia, L. Novel Turn-On Fluorescent Detection of Alkaline Phosphatase Based on Green Synthesized Carbon Dots and $MnO_2$ Nanosheets. *Talanta* **2017**, *165*, 136−142.
(25) Li, N.; Diao, W.; Han, Y.; Pan, W.; Zhang, T.; Tang, B. $MnO_2$-Modified Persistent Luminescence Nanoparticles for Detection and Imaging of Glutathione in Living Cells and in Vivo. *Chem. - Eur. J.* **2014**, *20*, 16488−16491.
(26) Huang, Z.; Cai, Q.; Ding, D.; Ge, J.; Hu, Y.; Yang, J.; Zhang, L.; Li, Z. A Facile Label-Free Colorimetric Method for Highly Sensitive Glutathione Detection by Using Manganese Dioxide Nanosheets. *Sens. Actuators, B* **2017**, *242*, 355−361.
(27) Yin, H.; Wang, M.; Zhou, Y.; Zhang, X.; Sun, B.; Wang, G.; Ai, S. Photoelectrochemical Biosensing Platform for MicroRNA Detection Based on in Situ Producing Electron Donor from Apoferritin-Encapsulated Ascorbic Acid. *Biosens. Bioelectron.* **2014**, *53*, 175−181.
(28) Meng, H.; Lu, L.; Zhao, X.; Chen, Z.; Zhao, Z.; Yang, C.; Zhang, X.; Tan, W. Multiple Functional Nanoprobe for Contrast-Enhanced Bimodal Cellular Imaging and Targeted Therapy. *Anal. Chem.* **2015**, *87*, 4448−4454.
(29) Zheng, F. F.; Wu, J. F.; Zhao, G. C. Peptide-Quantum Dot Bioconjugates for Label-Free Trypsin Detection Based on the Exciton Energy Transfer. *Anal. Methods* **2012**, *4*, 3932−3936.
(30) Ghosh, S.; Mohapatra, S.; Thomas, A.; Bhunia, D.; Saha, A.; Das, G.; Jana, B.; Ghosh, S. Apoferritin Nanocage Delivers Combination of Microtubule and Nucleus Targeting Anticancer Drugs. *ACS Appl. Mater. Interfaces* **2016**, *8*, 30824−30832.
(31) Atchudan, R.; Edison, T.; Aseer, K.; Perumal, S.; Karthik, N.; Lee, Y. Highly Fluorescent Nitrogen-Doped Carbon Dots Derived From Phyllanthus Acidus Utilized as a Fluorescent Probe for Label-Free Selective Detection of $Fe^{3+}$ Ions, Live Cell Imaging and Fluorescent Ink. *Biosens. Bioelectron.* **2018**, *99*, 303−311.
(32) Yan, X.; Song, Y.; Zhu, C.; Song, J.; Du, D.; Su, X.; Lin, Y. Graphene Quantum Dot-$MnO_2$ Nanosheet Based Optical Sensing Platform: a Sensitive Fluorescence "Turn Off-On" Nanosensor for Glutathione Detection and Intracellular Imaging. *ACS Appl. Mater. Interfaces* **2016**, *8*, 21990−21996.
(33) He, D.; Yang, X.; He, X.; Wang, K.; Yang, X.; He, X.; Zou, Z. A Sensitive Turn-On Fluorescent Probe for Intracellular Imaging of Glutathione Using Single-Layer $MnO_2$ Nanosheet-Quenched Fluorescent Carbon Quantum Dots. *Chem. Commun.* **2015**, *51*, 14764−14767.
(34) Borgström, A.; Andren-Sandberg, A. Elevated Serum Levels of Immunoreactive Anionic Trypsin (but Not Cationic Trypsin) Signals Pancreatic Disease. *Int. J. Pancreatol.* **1995**, *18*, 221−225.
(35) Wang, X.; Wang, Y.; Rao, H.; Shan, Z. A Sensitive Fluorescent Assay for Trypsin Activity in Biological Samples Using BSA-Au Nanoclusters. *J. Braz. Chem. Soc.* **2012**, *23*, 2011−2015.


DOI: 10.1021/acsabm.8b00235
*ACS Appl. Bio Mater.* 2018, 1, 777−782